Nanotechnology Perceptions
ISSN 1660-6795
www.nano-ntp.com

Influence of Divalent (Ca^{2+}) Substitution at Sr^{3+} site on Dielectric, Impedance and Conductive Response of Sr-M Solid Solutions

Pankaj Kumar

Department of Physics, RR BAWA DAV College, Batala, Punjab, India,
pguptahp78@gmail.com

Divalent metal ion (Ca^{2+}) modified Sr-M strontium hexaferrite $SrFe_{12}O_{19}$ Nano ceramic solid solutions ($Sr_{1-x}Ca_xFe_{12}O_{19}$, where x = 0.10, 0.50 & 0.60) have been synthesized using solid solutions. Prepared solid solution particles have been characterized for dielectric, impedance and conductivity response. Effect of temperature on dielectric, impedance and conductive behavior in frequency range varied from 100 Hz to 1 MHz have been analyzed and reported. The thermally activated hopping mechanism responsible for tailoring dielectric and impedance response have been analyzed. The effect of temperature results in creation of oxygen vacancies led improvement in conductivity has been recorded and reported. The increment in conductivity has also be confirmed from decrease in resistive response of prepared ceramic solid solutions. The maxima in imaginary part of impedance and electrical modulus evident for appearance of relaxation phenomenon. The shift in maxima with varying frequency towards higher frequency responsible for presence of frequency dependent dielectric relaxation in divalent substituted at Sr^{3+} in $SrFe_{12}O_{19}$ solid solutions. The conductivity behavior has been analyzed using universal power law
$\sigma_{ac}(\omega) = \sigma_{dc}(\omega) + A\omega^n$, where ωis frequency of applied signal of ac field, and n = exponent. $\sigma_{dc}(\omega)$ is commonly known as dc conductivity. The conduction mechanisms are mainly based on polaron hopping conduction. The dielectric and impedance properties of the prepared strontium hexaferrite samples were discussed in view of applications for microwave devices, permanent magnets and high frequency magnetic recording media.

Keywords: Hexaferrite, Hopping, Dielectric Relaxation, Space Charge Polarization, Conductivity.

1. Introduction

Hexaferrites are a class of ferrimagnetic materials known for their unique crystal structures and exceptional magnetic properties, making them vital components in various electronic and microwave applications. These materials, typically composed of iron oxides combined with other metal oxides like Ba^{2+}, Sr^{3+} or Pb^{2+}, exhibit complex magnetic behavior due to their hexagonal crystal structure. However, beyond their magnetic properties, hexaferrites also possess intriguing dielectric characteristics, which have garnered significant attention in recent years. Ferrites are especially belongs to ferrimagnetic ceramic materials made of two uneven sub-lattices of iron and another metal that are arranged anti-parallel to one another. At normal temperature, magnetization of hexagonal ferrites may result due to spontaneous magnetization is present in every sub lattice. The magnetization is comparable to ferromagnetic due to the uneven magnitudes. Ferrites exhibit magnetic saturation and hysteresis, have spontaneously magnetized domains, and have a critical temperature, T_c, also known as the Curie temperature, above which they magnetic ordering of ferrites get converted into paramagnetic. Because of these factors, polycrystalline ferrites are in high demand as excellent dielectric materials and as materials that are also very helpful for microwave devices. Ferrites characteristics are known to be highly influenced by their composition, synthesis process, temperature, frequency, and sintering conditions. Dielectric properties of hexaferrites are critical for their performance in high-frequency applications, such as microwave absorbers, antennas, and high-density data storage devices. These properties are influenced by factors like chemical composition, sintering temperature, grain size, and the presence of impurities. Understanding the dielectric behavior of hexaferrites, including their dielectric constant, loss tangent, and conductivity, is essential for optimizing their performance in various applications especially in microwave absorbing as well as antennas.

Dielectric spectroscopy and impedance spectroscopy are pivotal analytical techniques used to probe the electrical properties of materials across a wide frequency range. These methods are particularly valuable in the characterization of dielectric materials, polymers, biological tissues, and complex systems like electrolytes and composites. The analysis of dielectric properties and impedance responses enables researchers to gain deep insights into charge transport, polarization mechanisms, and molecular dynamics, which are critical for various applications in electronics, energy storage, and biomedical fields. Dielectric spectroscopy measures the dielectric permittivity of a material as a function of frequency, providing a direct assessment of its ability to store electrical energy and polarize in response to an applied electric field. This technique is crucial for understanding polarization mechanisms, including dipole orientation, ionic conductivity, and interfacial polarization, which are essential in the development of high-performance dielectric materials and capacitors whereas Impedance spectroscopy, on other hand, extends analysis by evaluating the complex impedance of a material, which includes both resistive and reactive components. By modeling the impedance data using equivalent circuits, researchers can dissect the contributions of bulk material properties, grain boundaries, and electrode interfaces, offering a comprehensive understanding of the material's electrochemical behavior. This method is instrumental in the study of batteries, fuel cells, and other electrochemical devices where ion transport and electrochemical reactions are of paramount importance. The integration of dielectric and impedance spectroscopy provides a robust framework for the detailed analysis of material properties,

enabling the development of innovative materials with tailored electrical characteristics. This paper aims to explore the fundamental principles of dielectric and impedance spectroscopy, their applications, and recent advancements in these techniques. By highlighting key case studies and current research trends, we seek to underscore the importance of these methods in advancing material science and engineering. Due to their many uses in electric motors, magnetic heads, high density recording media, microwave devices, and magneto-optic media, M-type hexaferrite (M = Ba, Sr, and Pb) crystallizes in a magneto-plumbite structure and is a class of significant magnetic materials. Ferrites are utilized in alternating magnetic fields from the perspective of microwave devices due to their superior magnetic properties at high frequencies, reduced eddy current loss, and high electrical resistance as compared to metal magnetic materials. Ferrite's composition and microstructure, which are influenced by processing conditions, are discovered to have an impact on its structural, magnetic, and electrical characteristics. The impact of finite size on the magnetic and structural characteristics of ferrite nanoparticles have been the subject of several investigations. Grain size, content, sintering temperature, and synthesis circumstances all affect the characteristics of these important dielectric materials. Two $SrFe_{12}O_{19}$ molecules make up their unit cell, which has 64 ions spread over 11 distinct symmetry points. Three octahedral sites—2a (up), 12 k (up), and 4f2 (down)—one tetrahedral site—4f1 (down), and one bipyramidal site—2b (up)—are home to the 24 Fe^{3+} ions where the spin orientations of Fe^{3+} ions are indicated by up and down. The distribution of the substituted cations at the five distinct crystallographic sites, based on their site preference, has a significant impact on these characteristics. Strontium hexa-ferrites are well-known for their superior magnetic properties, high Curie temperature, high electrical resistivity, low eddy current losses, excellent corrosion resistance, high chemical stability, low production costs, and non-toxicity. Because of these superior qualities, strontium hexaferrite can be used in high frequency applications [1-13].

This paper aims to explore the principles, methodologies, and applications of dielectric and impedance spectroscopy, providing a comprehensive overview of how these techniques contribute to advancing our understanding of material properties and their potential for technological innovations. In this paper, substitution of Ca^{2+} at Sr^{3+} site in $SrFe_{12}O_{19}$ (Sr-M) has been reported. The prepared ceramic solid solutions have been characterized for dielectric, impedance and conductive behavior at various temperature above RT (~273 K). The aim of such type of analysis to explore prepared ceramic solid solution important for various applications such as high-performance dielectric materials and capacitors.

2. Experimental Methodology:

Dielectric ceramics solid solutions of divalent metal ion (Ca^{2+}) substituted Sr-M strontium hexaferrite $SrFe_{12}O_{19}$ Nano ceramic solid solutions ($Sr_{1-x}Ca_xFe_{12}O_{19}$, where x = 0.10, 0.50 & 0.60) have been synthesized using solid solutions. Effect of valance state difference on dielectric and conductivity of prepared solid solutions have been characterized and reported. The valence state difference of parent & substituted Metal ion (Sr^{3+} & Ca^{2+}) led creation of oxygen vacancies which responsible for increase in conductivity of prepared solid solutions. The various metal ions required as per stoichiometric formula mentioned above weighed in required proportion. All weighed metal ion ions mixed first using motor pestle and then

transferred in bottles contains zirconia ball and mixed thoroughly using milling machine. The milling process has been carried out for 12 hours. After completion of milling process, mixed powder taken out from bottles and left for drying. The dried powder calcined at ~1000 °C for 12 hours for phase formation. The calcined powder mixed with 2% wt polyvinyl alcohol (PVA) as binder and pressed into circular disc of ~ 8 mm (diameter) & ~ 0.5 mm thick and sintered at 1200 °C for 2 hours for densifications. Sintered pellets have been characterized for various electric properties such as dielectric, impedance as well conductive behavior. For this, a conducting electrode has been deposited on circular disc for electric properties measurements.

Complex Impedance Spectroscopy

Complex Impedance Spectroscopy (CIS) is a very useful and significant characterizing technique in material science to study different electrical properties, such as real and imaginary parts of electrical impedance, real and imaginary parts of dielectric permittivity, contribution of grain and grain boundaries in electrical properties by studying Nyquist plots, and conduction mechanism from universal johncher's power fitting of conductivity data at various temperatures. For this, Z vs. θ at different temperatures have been recorded using impedance analyzer E4990A from KEYSIGHT TECHNOLOGIES, India and furnace from JUPITER ENGNEERING WORKS NEW DELHI interfaced with each other. The other parameters such as Z', ε', and Z'', ε'' & σ_{ac} etc. have been calculated from Z & θ using standard formulae.

The impedance analyzer (E4990A) from Keysight Technologies was used to determine these electrical characteristics. Using established equations, all of these parameters were computed from empirically acquired Z versus. θ at different temperatures

$$\text{Complex Impedance, } Z^* = Z' - jZ''$$

$$\text{Complex dielectric constant, } \varepsilon^* = \varepsilon' - j\varepsilon''$$

$$\text{Complex electric modulus, } M^* = M' + jM''$$

$$\text{Also, } \tan\delta = \frac{\varepsilon''}{\varepsilon'}$$

Where Z',ε', M' and Z'', ε'', M''denote the real and imaginary parts of the impedance, dielectric constant and electric modulus respectively and j = $\sqrt{(-1)}$. Studying the conduction process using Jonscher's power law [14];

$$\sigma_{ac} = \sigma_{dc} + A\omega^n$$

Where "n" is a dimensionless parameter that provides information on the interaction between mobile ions and the lattice in which they interact, "ac" stands for "ac conductivity," "dc" for "dc conductivity," "A" stands for the dispersion parameter expressing the strength of Polarizability, and so on. Dielectric relaxation is indicated by the maxima in Z" & M" vs. Frequency.

3. Results & Discussion

Figures 1 & 2 illustrate temperature-dependent ε' & ε" vs. frequency profile within frequency

range of 100-1MHz from 298K – 548K of Dielectric ceramics solid solutions of divalent metal ion (Ca^{2+}) substituted Sr-M strontium hexaferrite $SrFe_{12}O_{19}$ Nano ceramic solid solutions ($Sr_{1-x}Ca_xFe_{12}O_{19}$, where x = 0.10, 0.50 & 0.60). The real and imaginary part of dielectric permittivity has been calculated from impedance (Z) and phase angle (θ) using formulae given below

$$\varepsilon' = \frac{Z''}{\omega C_o (Z'^2 + Z''^2)}$$

$$\varepsilon'' = \frac{Z'}{\omega C_o (Z'^2 + Z''^2)}$$

The change in value of dielectric permittivity (Both real & Imaginary) as frequency increases (Descending Response) in prepared samples resembles to behaviors which commonly observed and reported in normal dielectrics. The regular decreasing trend (decrease of dielectric permittivity with frequency upto certain higher value of frequency and then become independent against frequency) may results due to extent of contribution of various polarizations in different range of frequency. It has been clearly visualized from graphs that prepared dielectric solid solutions exhibits maximum value of real & imaginary part of dielectric permittivity upto ~500 Hz (lower frequency regime) and then continuously decrease continuously with increasing frequency upto 5000 Hz and then responds independently to frequency of applied signal of ac electric field. The existence of all polarizations (ionic, dipolar, electronic, and space charge polarization) in lower frequency regime contributes in value of dielectric causes maximum in maximum value of real parts (ε' & ε'') reaches its maximum value but frequency starts increasing towards higher frequency regimes, elimination of some of polarizations mentioned get started and only space charge polarization responsible for linear variation of dielectric permittivity. The figures make it quite evident that value of dielectric permittivity (ε') initially rises to a specific values for particular highest temperature before falling. This kind of trend can be explained by the hypothesis that the initial increase may be the result of dipoles being easily orientated with respect to the applied field because they have received enough energy to do so or enough energy to overcome the thermal barrier, which is energy from external heat. Outside of this temperature range, temperature-dependent dielectric relaxation occurs because dipole becomes unable to responds against frequency of applied electric field appropriately. Theoretical models of such as Debye or non-Debye relaxation model have been applied to experimentally collected dielectric data in order to further investigate the possibility of dielectric relaxation either it may Debye or non-Debye relaxation. [15–19]. After first increasing to a specific temperature, the true dielectric permittivity value begins to drop. The thermal energy that dipoles receive from heating can be responsible for this kind of behavior which made dipoles so efficient that they can easily respond to external applied electric field results in increase in value of dielectric constant

$$\varepsilon'(\omega) = \varepsilon_\infty + (\varepsilon_s - \varepsilon_\infty)\frac{1 + (\omega\tau_0)^{1-\alpha}\sin\frac{\alpha\pi}{2}}{1 + 2(\omega\tau_0)^{1-\alpha}\sin\frac{\alpha\pi}{2} + (\omega\tau_0)^{2(1-\alpha)}}$$

$$\varepsilon''(\omega) = (\varepsilon_s - \varepsilon_\infty)\frac{(\omega\tau_0)^{1-\alpha}\cos\frac{\alpha\pi}{2}}{1 + 2(\omega\tau_0)^{1-\alpha}\sin\frac{\alpha\pi}{2} + (\omega\tau_0)^{2(1-\alpha)}}$$

where ε_∞ = dielectric constant measured at high frequency, ε_s = dielectric constant measured at low frequency, $\omega = 2\pi f$ the angular frequency of applied field and τ = characteristics relaxation time of the medium. The exponent parameter α usually varies between 0 and 1, and it describes the shape of spectral curves. It may be noted that for $\alpha = 0$, the Cole-Cole model reduces to the Debye model.

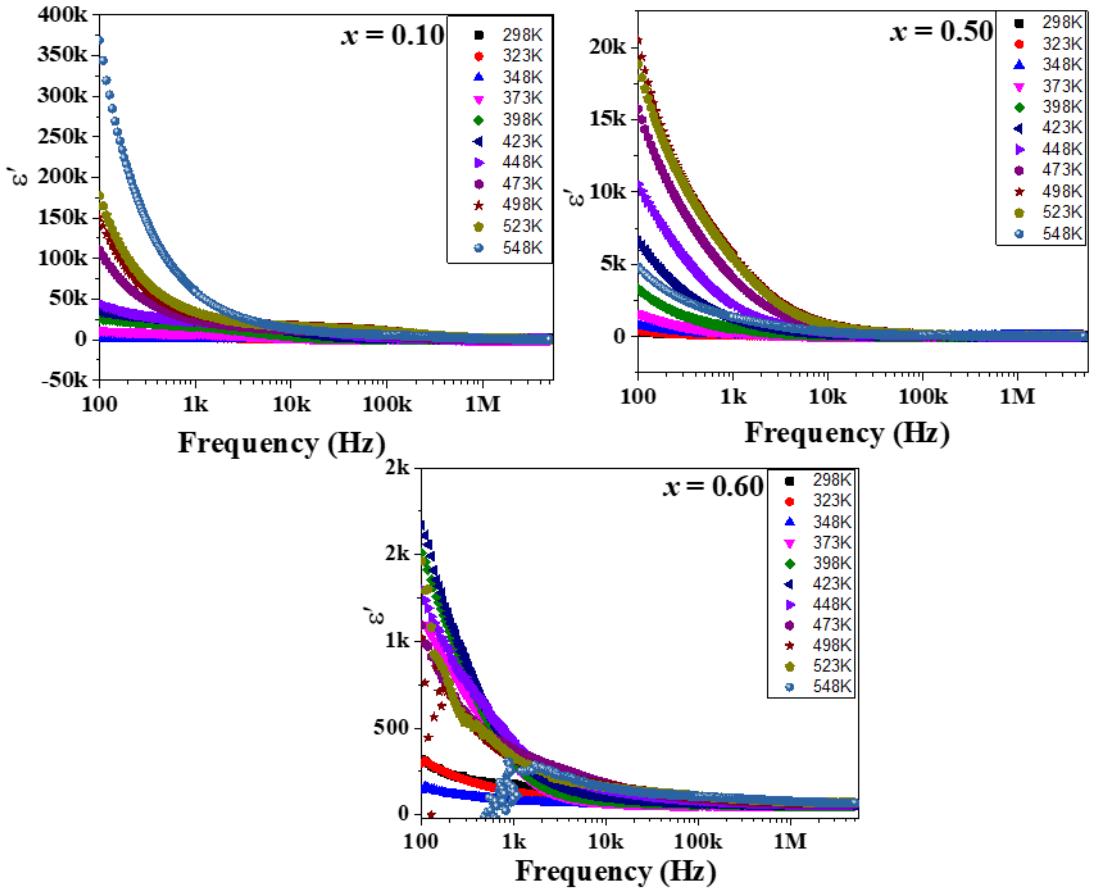

Figure 1: ε' vs Frequency (100Hz – 1 MHz) in temperature range varied from 298K-548K of divalent metal ion (Ca^{2+}) substituted Sr-M strontium hexaferrite $SrFe_{12}O_{19}$ Nano ceramic solid solutions ($Sr_{1-x}Ca_xFe_{12}O_{19}$, where x = 0.10, 0.50 & 0.60)

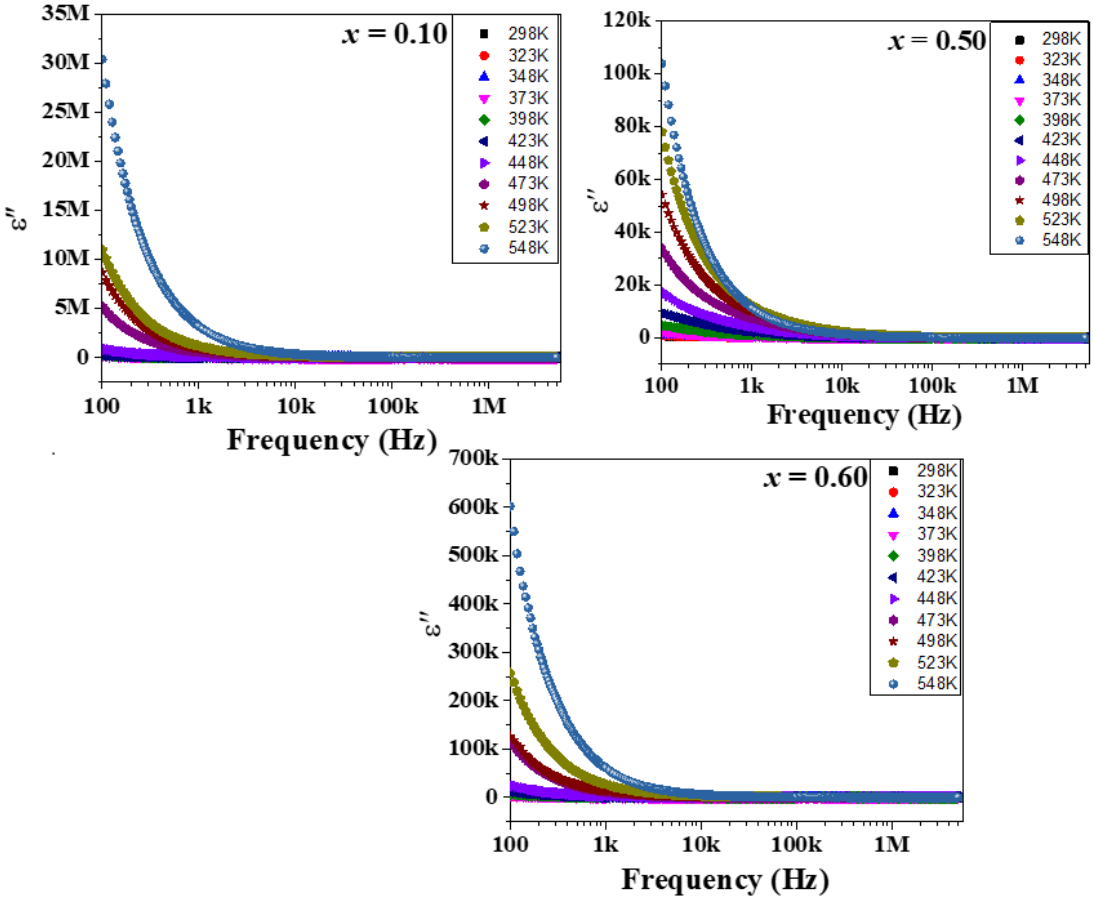

Figure 2: ε" vs Frequency (100Hz – 1 MHz) in temperature range varied from 298K-548K of divalent metal ion (Ca^{2+}) substituted Sr-M strontium hexaferrite $SrFe_{12}O_{19}$ Nano ceramic solid solutions ($Sr_{1-x}Ca_xFe_{12}O_{19}$, where x = 0.10, 0.50 & 0.60)

Figure 3 display Z′ vs. Frequency (Hz) profile within frequency range of 100-1MHz from 298K – 548K of Dielectric ceramics solid solutions of divalent metal ion (Ca^{2+}) substituted Sr-M strontium hexaferrite $SrFe_{12}O_{19}$ Nano ceramic solid solutions ($Sr_{1-x}Ca_xFe_{12}O_{19}$, where x = 0.10, 0.50 & 0.60). Real part of impedance has been calculated from Z and phase angle (θ) using formula given below

$$Z' = |Z|\cos(\theta)$$

It has been clearly delineated from graph that as frequency and temperature both increases simultaneously, Z′ decreases proclaimed an increase in conductivity in prepared Sr-M hexagonal ferrites. The decrease in value of Z′ with increasing temperature continuously evident for presence of negative temperature coefficient of resistance (NTCR) [13]. This increase of conductivity may also due to increase in concentration of oxygen vacancies which may results either due to sintering in air deficient environment as well as difference in valance state of substituents and parent ion. This increase in concentration of oxygen due to partial

substitution of Sr^{3+} with Ca^{2+} results in decreased value of Z´ directly proclaimed for reduction in resistive properties followed by increasing conductive behavior in prepared ceramic dielectric solid solution. The decreased resistive behavior or barrier can also be justified from temperature dependent conductivity profile. The increase in conductivity with temperature may results due to increase in concentration of oxygen vacancies with increasing temperature. The decreased trend in value of Z´with increasing both temperature and frequency may also confirmed from an increase in ac conductivity [20-21].The magnitude of Z´ merges after particular value of frequency in higher frequency region at all temperatures may also due to release of space charges which reduces the barrier properties in the materials. The increase in concentration of hopping charges created by increase in concentration of substituent (Ca^{2+}) may also responsible for decrease in impedance properties caused by space charge polarization which responsible for net dielectric constant in higher frequency region.

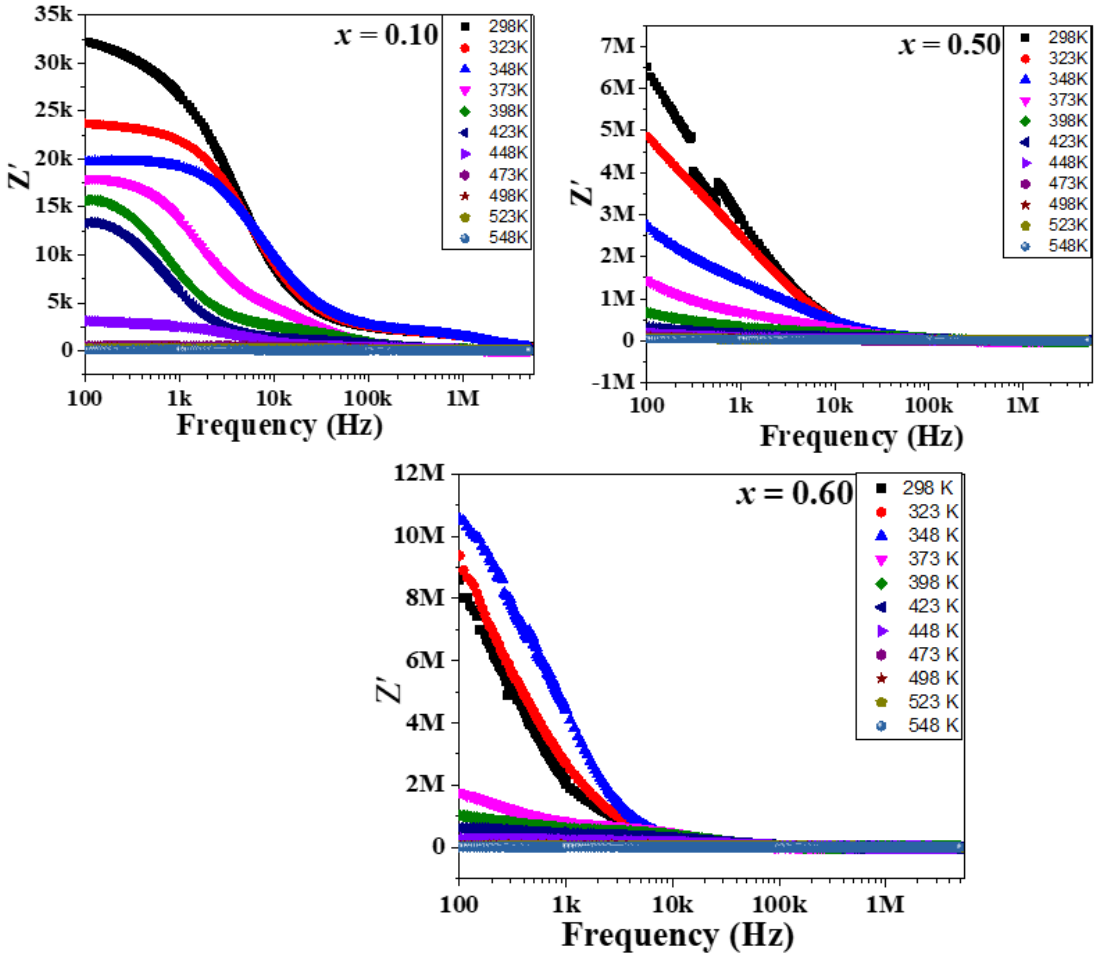

Figure 3: Z´ vs. Frequency (Hz) profile (100Hz – 1 MHz) in temperature range varied from 298K-548K of divalent metal ion (Ca^{2+}) substituted Sr-M strontium hexaferrite $SrFe_{12}O_{19}$ Nano ceramic solid solutions ($Sr_{1-x}Ca_xFe_{12}O_{19}$, where x = 0.10, 0.50 & 0.60)

The maxima in $Z^{''}$ vs. frequency shows appearance of resonance in prepared ceramic solid solutions. When frequency of externally applied electric field resonates with frequency of ion, maxima commonly known as resonance behavior arises. This resonance behavior may be due to exchange of energy in hopping of Fe^{3+} & Fe^{2+} which results due to difference in valance state of substituent and parent metal ion and increases as concentration of substituent increases causes energy loss due to the high resistance of grain boundaries. Figure 4 display $Z^{'}$ vs. Frequency (Hz) profile within frequency range of 100-1MHz from 298K – 548K of Dielectric ceramics solid solutions of divalent metal ion (Ca^{2+}) substituted Sr-M strontium hexaferrite $SrFe_{12}O_{19}$ Nano ceramic solid solutions ($Sr_{1-x}Ca_xFe_{12}O_{19}$, where x = 0.10, 0.50 & 0.60). Real part of impedance has been calculated from Z and phase angle (θ) using formula given below

$$Z^{''} = |Z|\sin(\theta)$$

It has been clearly seen from graphs that value of imaginary part of impedance ($Z^{''}$) first increases continuously with increasing frequency and achieved maximum value and then starts decreases with continuous increase in frequency. The maxima of $Z^{''}$ at particular frequency known as resonance frequency at which frequency of ion resonates with frequency of externally applied electric field clearly reveals presence dielectric relaxations. The continuous shift in maxima of $Z^{''}$ with Frequency as well as temperature evident for presence of frequency and temperature dependent dielectric relaxation. The disappearing of maxima in value of imaginary part of impedance (merging at higher temperatures) reveals for elimination of space charge polarization [22-24].

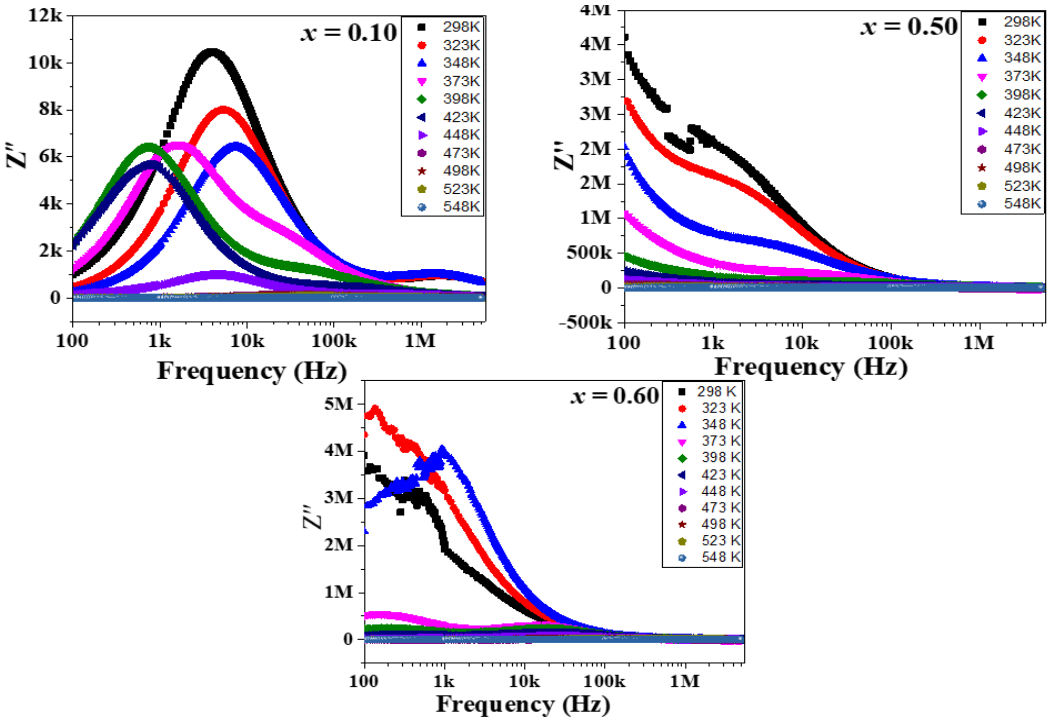

Figure 4: $Z^{''}$ vs. Frequency (Hz) profile (100Hz – 1 MHz) in temperature range varied from 298K-548K of divalent metal ion (Ca^{2+}) substituted Sr-M strontium hexaferrite $SrFe_{12}O_{19}$

Nano ceramic solid solutions ($Sr_{1-x}Ca_xFe_{12}O_{19}$, where x = 0.10, 0.50 & 0.60)

Dielectric Relaxation has also be analyzed from frequency dependence plots of $M^{''}$at different temperature. Figure 5 display $M^{''}$ vs. Frequency (Hz) profile within frequency range of 100-1MHz from 298K – 548K of Dielectric ceramics solid solutions of divalent metal ion (Ca^{2+}) substituted Sr-M strontium hexaferrite $SrFe_{12}O_{19}$ Nano ceramic solid solutions ($Sr_{1-x}Ca_xFe_{12}O_{19}$, where x = 0.10, 0.50 & 0.60). Imaginary part of electrical modulus has been calculated from Z and phase angle (θ) using formula given below

$$M'' = \omega C_o Z'$$

Where Z' is real part of impedance. It has been clearly depicted from graph that as frequency increases towards its high regime along with continuous increment in temperature, position of maxima (resonance frequency) in M'' vs. frequency profiles ($M^{''}_{max}$) has been continuously shifted towards high frequency region gives direct evidence for presence of temperature dependent hopping mechanism in electrical conduction. The non-Debye nature of dielectric relaxation with different time constant for relaxation response resulted from asymmetric broadening of the peak [22, 25]. The maxima of M'' vs. frequency profiles ($M^{''}_{max}$) in lower frequency regions claims of long range mobility of the ions whereas maxima of M'' vs. frequency profiles ($M^{''}_{max}$) peaks in high frequency regime reveals confinement of ions in potential wells within shorter distances range [26].

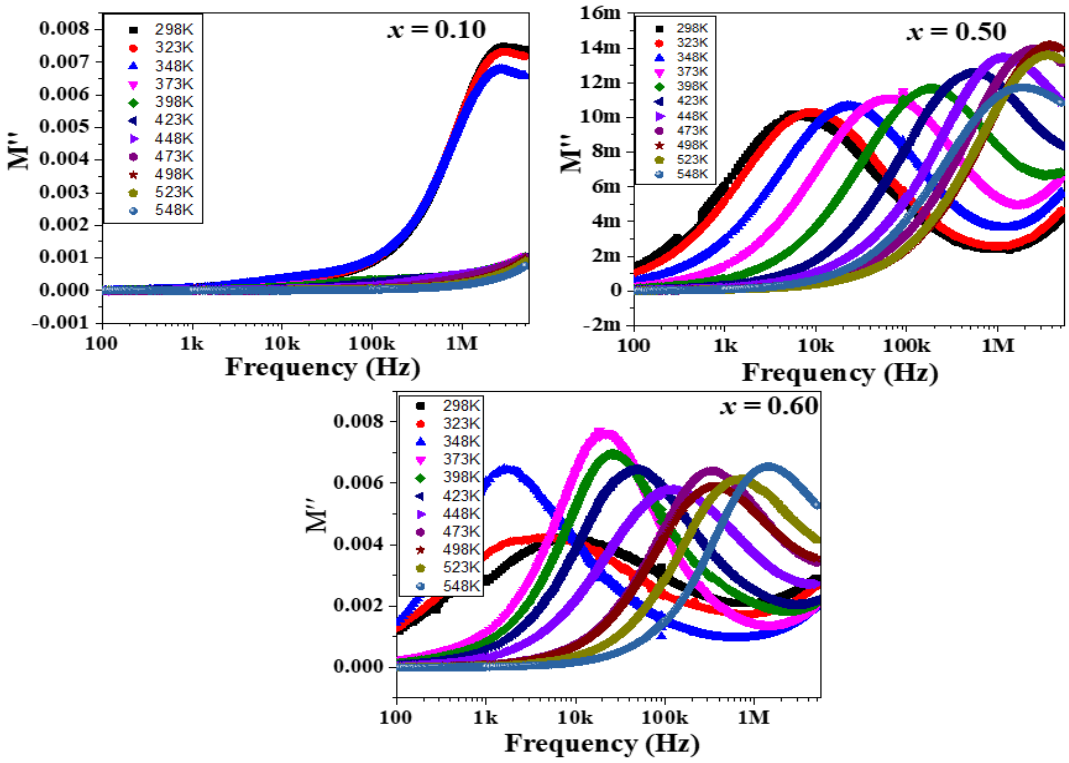

Figure 5: M'' vs. frequency profiles ($M^{''}_{max}$) (100Hz – 1 MHz) in temperature range varied from 298K-548K of divalent metal ion (Ca^{2+}) substituted Sr-M strontium hexaferrite

$SrFe_{12}O_{19}$ Nano ceramic solid solutions ($Sr_{1-x}Ca_xFe_{12}O_{19}$, where x = 0.10, 0.50 & 0.60)

Influence of divalent substitution (Ca^{2+}) at trivalent Sr^{3+} site on conductive response of Sr-M hexaferrite has been analyzed from σ_{ac} vs. Frequency (Hz). ac conductivity (σ_{ac}) has been calculated from dielectric parameters using formula given below

$\sigma_{ac} = 2\pi f \varepsilon' \varepsilon_o \tan\delta$

Figure 6 displayM'' vs. Frequency (Hz) profile within frequency range of 100-1MHz from 298K – 548K of Dielectric ceramics solid solutions of divalent metal ion (Ca^{2+}) substituted Sr-M strontium hexaferrite $SrFe_{12}O_{19}$ Nano ceramic solid solutions ($Sr_{1-x}Ca_xFe_{12}O_{19}$, where x = 0.10, 0.50 & 0.60). It has been clearly seen in graphs that graphs divided into two parts (a) frequency independence represents to dc conductivity (σ_{dc}) & (b) varied w.r.t. frequency in higher frequency regime termed as ac conductivity (σ_{ac}). The universal johncher's power law has been used to study conduction mechanism from ac conductivity given as follow

$$\sigma_{ac} = \sigma_{dc} + A\omega^n$$

Where σ_{ac} = ac conductivity, σ_{dc} = dc conductivity, A = dispersion parameter representing the strength of Polarizibilty & "n" is dimensionless parameter.

It has been clearly perceived from graphs that conductivity increases with increasing temperature. The increase of oxygen vacancies due to temperature may results for uninterrupted increase in electrical conductivity. [27-29].

4. Conclusion

Divalent metal ion (Ca^{2+}) substituted Sr-M strontium hexaferrite $SrFe_{12}O_{19}$ Nano ceramic solid solutions ($Sr_{1-x}Ca_xFe_{12}O_{19}$, where x = 0.10, 0.50 & 0.60) have been synthesized using mechanical mixing method. Dielectric permittivity's real as well as imaginary component first rises to a specific temperature before beginning to fall. This indicates that dipoles receive enough energy from the temperature to react to applied signals easily, while a further decline indicates that dipoles are unable to do so. As the temperature and Ca^{2+} concentration rise, real part of the electrical impedance parameter falls. This is directly related to the electrical conductivity behavior which also get enhanced. The enhancement or increased in value of electric conductivity strongly stamped for increase in concentration of oxygen vacancies. The valance state difference of substituent and parent metal ion and sintering in oxygen deficient environment responsible for increase in concentration of oxygen vacancies.

References

1. Guolong Tann, Xiuna Chen, Structure and multiferroic properties of barium hexaferrite ceramics, Journal of Magnetism and Magnetic Materials 327 (2013) 87–90
2. Meera Rawat and K L Yadav, Electrical, magnetic and magnetodielectric properties in ferrite-ferroelectric particulate composites, IOP Publishing, Smart Materials and Structures, Smart Mater. Struct. 24 (2015) 045041 (11pp) doi:10.1088/0964-1726/24/4/045041
3. Ayesha Khalid, Ghulam M. Mustafa, Shahzad Naseem, Shahid Atiq, Sm-mediated dielectric characteristics and tunable magneto-electric coefficient of 0.5Bi1-xSmxFe0.95Mn0.05O3-

0.5PbTiO3 composites, Ceramics International 45 (2019) 7690-7695
4. Kanchan Bala, R.K. Kotnalab, N.S. Negi, Magnetically tunable dielectric, impedance and magnetoelectric response in MnFe2O4/(Pb1−xSrx)TiO3 composites thin films, Journal of Magnetism and Magnetic Material, 424 (2017), 256-266
5. Himani Joshi, A. Ruban Kumar, Investigations and Correlations of Structural, Magnetic, and Dielectric Properties of M Type Barium Hexaferrite (BaFe12O19) for Hard Magnet Applications, Journal of Superconductivity and Novel Magnetism (2022) 35:2435–2451 https://doi.org/10.1007/s10948-022-06203-x
6. Khomskii DI (2006) Multiferroics: Different ways to combine magnetism and ferroelectricity. J Magn Magn Mater 306:1–8. https://doi.org/10.1016/j.jmmm.2006.01.238
7. Spaldin NA, Fiebig M (2005) The Renaissance of Magnetoelectric Multiferroics. Mater Sci 309:391–392
8. Eerenstein W, Mathur ND, Scott JF (2006) Multiferroic and magnetoelectric materials. Nature 442:759–765. https://doi.org/10.1038/nature05023
9. Guolong Tann, Xiuna Chen, Structure and multiferroic properties of barium hexaferrite ceramics, Journal of Magnetism and Magnetic Materials 327 (2013) 87–90
10. Meera Rawat and K L Yadav, Electrical, magnetic and magnetodielectric properties in ferrite-ferroelectric particulate composites, IOP Publishing, Smart Materials and Structures, Smart Mater. Struct. 24 (2015) 045041 (11pp) doi:10.1088/0964-1726/24/4/045041
11. Ayesha Khalid, Ghulam M. Mustafa, Shahzad Naseem, Shahid Atiq, Sm-mediated dielectric characteristics and tunable magneto-electric coefficient of 0.5Bi1-xSmxFe0.95Mn0.05O3-0.5PbTiO3 composites, Ceramics International 45 (2019) 7690-7695
12. Kanchan Bala, R.K. Kotnalab, N.S. Negi, Magnetically tunable dielectric, impedance and magnetoelectric response in MnFe2O4/(Pb1−xSrx)TiO3 composites thin films, Journal of Magnetism and Magnetic Material, 424 (2017), 256-266
13. Himani Joshi, A. Ruban Kumar, Investigations and Correlations of Structural, Magnetic, and Dielectric Properties of M Type Barium Hexaferrite (BaFe12O19) for Hard Magnet Applications, Journal of Superconductivity and Novel Magnetism (2022) 35:2435–2451 https://doi.org/10.1007/s10948-022-06203-x
14. Jonscher AK. The Universal dielectric response. Nature. 1977;267:673-679.
15. Tiku Ram, Akshay, Kanchan Khanna, Sunil K. Dwivedi and Sunil Kumar, Effect of Synthesis method on Structural, Ferroelectric and conduction relaxation in Pb1-xLaxTiO3, where x = 0.25 ceramics , Material Today Proceedings, Vol. 65 Part 1 (2022) 327-331, doi:10.1016/j.matpr.2022.06.206
16. Correlation between Sintering Temperature and Structural, Ferroelectric Properties of Pb0.75Nd0.25TiO3 Ceramics, Akshay Kumar, Tiku Ram, Kanchan Khanna, Sunil K. Dwivedi and Sunil Kumar, Material Today Proceedings, Vol. No. 65 Part 1(2022) 322-326
17. Kumar M, Yadav KL. J. Phys.: Condens. Matter. 2002;19:242202.
18. Cole KS, Robert H. Dispersion and Absorption in Dielectrics:- Alternating Current Characteristics. Journal of Chemical Physics. 1941;9:341–351.
19. Badapanda, T., Sarangi, S., Behera, B., Anwar, S. (2014). Structural and Impedance spectroscopy study of Samarium modified Zirconium Titanate ceramic prepared by mechanochemical route. Current Applied Physics, 14: 1192-1200.
20. Dash, U., Sahoo, S., Chaudhuri, P., Parashar, S.K.S., Parashar, K. (2014). Electrical properties of bulk and nano Li2TiO3 ceramics: A comparative study. Journal of Advanced ceramics. 3: 89-97.
21. Tiwari, B., Choudhary, R.N.P. (2010). Study of Impedance Parameters of Cerium Modified Lead Zirconate Titanate Ceramics. IEEE Transactions on Dielectrics and Electrical Insulation. 17: 5-17.
22. Badapanda, T., Sarangi, S., Behera, B.,Anwar, S. (2014). Structural and Impedance spectroscopy

study of Samarium modified Zirconium Titanate ceramic prepared by mechanochemical route. Current Applied Physics. 14: 1192-1200.

23. Biswal, M.R., Nanda, J., Mishra, N.C., Anwar, S., Mishra, A. (2014). Dielectric and impedance spectroscopic studies of multiferroic BiFe1-xNixO3. Advanced Materials Letter. 5: 531-537.
24. Rajan, R., Kumar, R., Behera, B., Choudhary, R.N.P. (2009). Structural and impedance spectroscopic studies of samarium modified lead zirconate titanate ceramics. Physica B. 404: 3709-3716.
25. Priyanka, Jha, A.K. (2015). Electrical characterization of zirconium substituted barium titanate using complex impedance spectroscopy. Bull. Mater. Sci, 36: 135-141.
26. Shukla, A., Choudhary, R.N.P. (2011). High temperature impedance and modulus spectroscopy characterization of La3+/Mn4+ modified PbTiO3nanoceramics. Physica B: Physics of condensed Mater, 406: 2492-2500.
27. Tan M, Koseoglu V, Alan F, Senturk E. Overlapping large Polaron tunneling conductivity and giant dielectric constant in Ni0.5Zn0.5Fe1.5Cr0.5O4 nanoparticles (NPs). J Alloys Compd. 2011;509:9399-9405.
28. Vaish R, Varma KBR. Dielectric properties of Li2O-3B2O3 glasses. J. Appl. Phys. 2009;103:064106.
29. Megdiche M, Pellegrino CP, Gargouri M. Conduction mechanism study by overlapping large Polaron tunneling model in SrNiP2O7 ceramic compound. J Alloys Compd. 2014;584:209-215.